June 1993 Journal Article

HYPERVELOCITY ORBITAL INTERCEPT GUIDANCE USING CERTAINTY CONTROL

PR: 9993
TA: LA
WU: BS

Salvatore Alfano and Charles E. Fosha Jr.

United States Air Force Academy
Colorado Springs, Colorado 80840

Phillips Laboratory
3550 Aberdeen Avenue, SE
Kirtland AFB, NM 87117-5776

PL-TR--93-1020

Published by the Journal of Guidance, Control, and Dynamics, Vol. 14, No. 3, pp. 574-580.
Lt Col Alfano is presently assigned to PL/VTA, Kirtland AFB, NM 87117-5776.

Terminal guidance of a hypervelocity exoatmospheric orbital interceptor with free end time is examined. A new approach called certainty control is developed where control energy expenditure is reduced by constraining the expected final state to a function of projected estimate error. Conceptually, the constraint produces a shrinking sphere about the predicted impact point with the radius being a function of estimated error. If the predicted miss is inside or touching the sphere, thrusting is not necessary. The interceptor is modeled as a satellite with lateral thrusting capability using two-body orbital dynamics. The target is modeled as an intercontinental ballistic missile (IBM) in its final boost phase prior to burnout. Filtering is accomplished using an eight-state extended Kalman filter with line-of-sight and range updates. The estimated relative trajectory and variances are propagated numerically to predicted impact time and then approximated by splines, eliminating the need to propagate new data repeatedly when present conditions are varied. A search is then made for a new impact time and point that will minimize present interceptor velocity changes and final miss distance. This control strategy, which is applied to two intercept problems, substantially reduces fuel consumption.

thrust control, terminal guidance, guided missiles, weapon control, control theory, hypervelocity rockets, kinetic energy

8

Unclassified	Unclassified	Unclassified	SAR

Hypervelocity Orbital Intercept Guidance Using Certainty Control

Salvatore Alfano*
United States Air Force Academy, Colorado Springs, Colorado 80840
and
Charles E. Fosha Jr.†
University of Colorado, Colorado Springs, Colorado 80918

Terminal guidance of a hypervelocity exoatmospheric orbital interceptor with free end time is examined. A new approach called certainty control is developed where control energy expenditure is reduced by constraining the expected final state to a function of projected estimate error. Conceptually, the constraint produces a shrinking sphere about the predicted impact point with the radius being a function of estimated error. If the predicted miss is inside or touching the sphere, thrusting is not necessary. The interceptor is modeled as a satellite with lateral thrusting capability using two-body orbital dynamics. The target is modeled as an intercontinental ballistic missile (IBM) in its final boost phase prior to burnout. Filtering is accomplished using an eight-state extended Kalman filter with line-of-sight and range updates. The estimated relative trajectory and variances are propagated numerically to predicted impact time and then approximated by splines, eliminating the need to propagate new data repeatedly when present conditions are varied. A search is then made for a new impact time and point that will minimize present interceptor velocity changes and final miss distance. This control strategy, which is applied to two intercept problems, substantially reduces fuel consumption.

Nomenclature

A	= present acceleration, m/s^2
A_0	= initial acceleration, m/s^2
A,B,C,D	= coefficients of splines (A, m/s^3; B, m/s^2; C, m/s; D, m)
a_y,a_z	= lateral thrust accelerations, m/s^2
$d\Delta V_y$	= differential change in velocity change
E	= expected value operator
f	= scalar cost function
$G_{x\delta}$	= uncertainty in final state
H	= Hamiltonian, = cost function + constraint adjoined via Lagrangian multiplier
J	= Jacobian matrix of f vector
K	= constraint weighting factor
L	= cost function
m_0	= initial mass flow rate divided by mass, s^{-1}
R	= relative range, m
t	= current time, s
t_{go}	= time to go, s
V	= relative velocity, m/s
x_f	= final state
x_s	= predicted final state without control update using splines
$x,y,z_{I,T}$	= x, y, z coordinate positions for interceptor and target, m
$\Delta V_y,\Delta V_z$	= interceptor's velocity changes, m/s
λ	= Lagrangian multiplier
μ	= Earth's gravitational constant
σ	= standard deviation

Superscripts

$(^*)$	= denotes best estimate
$(\dot{})$	= denotes the first derivative with respect to time
$(\ddot{})$	= denotes the second derivative with respect to time

Received April 28, 1989; revision received Jan. 16, 1990.

*Associate Professor, Director of Research, Department of Astronautics. Senior Member AIAA.

†Associate Professor Attendant, Department of Electrical Engineering; Interim Director, Space Studies Program, Director of Space and Flight Systems Laboratory. Member AIAA.

Introduction

INTERCEPTOR performance can be enhanced by using a terminal guidance law that incorporates the dynamics of the interceptor and target plus the error knowledge of their estimates. This paper develops a guidance scheme that minimizes lateral thrusting for a hypervelocity, exoatmospheric orbital vehicle in the final 30 s of flight while it is attempting to intercept a boosting missile.

Much work has been done in the area of air-to-air guidance that has space-to-space application. Guelman[1,2] has derived a closed-form solution for pure proportional navigation. Singular perturbation methods have been employed by Sridhar and Gupta[3] for air-to-air guidance. Design procedures using optimal and stochastic control techniques abound.[4-14] In the works just cited, the force of gravity is assumed to act equally on the interceptor and target and is ignored in the relative dynamics. This flat-Earth assumption is adequate for air-to-air encounters, but not for space-to-space, except at short ranges. For orbital intercepts with large initial ranges, the force of gravity will affect the relative trajectory and should be included in the equations of motion.

The literature for space-to-space guidance reveals many numerical approaches for determining present velocity for future rendezvous.[15-21] To date, analytic solutions for such intercepts exist only when the interceptor's impact conditions are prespecified.[19] These works do not address hypervelocity intercept involving seconds, but are concerned with a much slower rendezvous process involving hours or even days.

The guidance scheme presented here attempts to minimize lateral velocity changes by varying the impact conditions through the use of splines. Splines were used by Johnson[16] in presenting a possible Earth-Mars transfer guidance algorithm. Dickmanns and Wells,[22] as well as Hargraves and Paris,[23] have used third-order polynomials for general trajectory optimization. The splines result in faster searches by eliminating the need to propagate new trajectories repeatedly when conditions are varied. This feature makes them attractive for a hyperve-

locity orbital intercept that requires a fast and reasonably accurate numerical search.

Target tracking is accomplished with a ranging device and line-of-sight sensors for in-plane and out-of-plane measurements. Noise-corrupted data is processed through an extended Kalman filter (EKF) with serial updates occurring every 0.1 s.

By constraining the estimated final state to a function of the projected estimate error, much needless thrusting can be eliminated in the presence of poor estimates. This strategy can substantially reduce the fuel consumption needed for intercepts.

System Modeling

Here, the equations of motion for the target and interceptor are developed. Atmospheric drag will not be considered in the dynamics because the interceptor is assumed exoatmospheric. Also, due to the interceptor's lateral thrusting limitation, the longitudinal axis will be assumed to be parallel to the interceptor's initial velocity vector.

The interceptor is modeled as a satellite traveling in excess of 12 km/s with lateral thrusting capability using two-body orbital dynamics. Thrusting is prohibited along the longitudinal (x) axis in the forward direction to prevent sensor contamination and in the rearward direction because of the large aft booster necessary to achieve hypervelocity speed. The equations of motion are as follows:

$$\ddot{x}_I = \frac{-\mu x_I}{(x_I^2 + y_I^2 + z_I^2)^{3/2}} \tag{1}$$

$$\ddot{y}_I = \frac{-\mu y_I}{(x_I^2 + y_I^2 + z_I^2)^{3/2}} + a_y \tag{2}$$

$$\ddot{z}_I = \frac{-\mu z_I}{(x_I^2 + y_I^2 + z_I^2)^{3/2}} + a_z \tag{3}$$

The target is modeled as an intercontinental ballistic missile (ICBM) in its final boost phase using two-body orbital dynamics. For tracking purposes, the intercept must occur prior to burnout. Acceleration due to thrusting is computed in the direction of the ICBM's velocity vector. The equations of motion are

$$A = \frac{A_0}{1 - \dot{m}_0 t} \tag{4}$$

$$\ddot{x}_T = \frac{-\mu x_T}{(x_T^2 + y_T^2 + z_T^2)^{3/2}} + \frac{A \dot{x}_T}{(\dot{x}_T^2 + \dot{y}_T^2 + \dot{z}_T^2)^{1/2}} \tag{5}$$

$$\ddot{y}_T = \frac{-\mu y_T}{(x_T^2 + y_T^2 + z_T^2)^{3/2}} + \frac{A \dot{y}_T}{(\dot{x}_T^2 + \dot{y}_T^2 + \dot{z}_T^2)^{1/2}} \tag{6}$$

$$\ddot{z}_T = \frac{-\mu z_T}{(x_T^2 + y_T^2 + z_T^2)^{3/2}} + \frac{A \dot{z}_T}{(\dot{x}_T^2 + \dot{y}_T^2 + \dot{z}_T^2)^{1/2}} \tag{7}$$

Problem Statement and Truth Model

Time-to-go and interceptor velocity changes are the control parameters that must be varied to minimize miss distance and fuel expended (i.e., velocity changes). The mathematical representation of this control objective is presented in the section on certainty control, which follows. Miss distance is determined by establishing a time remaining until intercept (time to go) and propagating the equations of motion forward. An iterative process can then be used to find the interceptor velocity needed to bring the miss distance to zero. The difference between current velocity and that needed for intercept, known as velocity to go, must be minimized. To accomplish this, the time to go is varied and the procedure just mentioned is repeated until a minimum velocity to go is found.

The computation of needed velocity is time consuming because the equations of motion are nonlinear and do not lend themselves to closed-form solution. These equations must be propagated numerically to intercept time whenever the initial velocity is varied. The previous method will serve as the basis (truth) model for this control problem using the numerical techniques found in Maron.[24]

A Newton-Raphson method for solving nonlinear systems is employed to determine the proper values of the control parameters. Let

$$u = \begin{bmatrix} \Delta V_y \\ \Delta V_z \\ t_{go} \end{bmatrix} \tag{8}$$

be a solution of the nonlinear system

$$\begin{bmatrix} f_1(u) \\ f_2(u) \\ f_3(u) \end{bmatrix} = \begin{bmatrix} x_T(t_{go}) - x_I(t_{go}) \\ y_T(t_{go}) - y_I(t_{go}) - \Delta V_y t_{go} \\ z_T(t_{go}) - z_I(t_{go}) - \Delta V_z t_{go} \end{bmatrix} = \begin{bmatrix} 0 \\ 0 \\ 0 \end{bmatrix} \tag{9}$$

The effect of small velocity changes in Eq. (9) can be considered linear because the interceptor is assumed to travel at hypervelocity, resulting in a near straight-line trajectory. Any error caused by this assumption will be accounted for in the succeeding iteration when the proposed velocity change is incorporated in the nonlinear dynamics.

The initial control values must be incrementally changed to satisfy Eq. (9). A linear approximation of the f vector for changes in u will yield approximate increments of the control parameters. The linearized system becomes

$$[J] \begin{bmatrix} d\Delta V_y \\ d\Delta V_z \\ dt_{go} \end{bmatrix} = - \begin{bmatrix} f_1(u) \\ f_2(u) \\ f_3(u) \end{bmatrix} \tag{10}$$

where J is the Jacobian matrix of the f vector evaluated at u:

$$[J] = \begin{bmatrix} 0 & 0 & \{\dot{x}_T(t_{go}) - \dot{x}_I(t_{go})\} \\ -t_{go} & 0 & \{\dot{y}_T(t_{go}) - \dot{y}_I(t_{go}) - \Delta V_y\} \\ 0 & -t_{go} & \{\dot{z}_T(t_{go}) - \dot{z}_I(t_{go}) - \Delta V_z\} \end{bmatrix} \tag{11}$$

To determine changes in the u vector, f is multiplied by the negative inverse of J

$$\begin{bmatrix} d\Delta V_y \\ d\Delta V_z \\ dt_{go} \end{bmatrix} = -[J]^{-1} \begin{bmatrix} f_1(u) \\ f_2(u) \\ f_3(u) \end{bmatrix} \tag{12}$$

$$[J]^{-1} = \begin{bmatrix} \dfrac{\dot{y}_T(t_{go}) - \dot{y}_I(t_{go}) - \Delta V_y}{\{\dot{x}_T(t_{go}) - \dot{x}_I(t_{go})\} t_{go}} & \dfrac{-1}{t_{go}} & 0 \\ \dfrac{\dot{z}_T(t_{go}) - \dot{z}_I(t_{go}) - \Delta V_z}{\{\dot{x}_T(t_{go}) - \dot{x}_I(t_{go})\} t_{go}} & 0 & \dfrac{-1}{t_{go}} \\ \dfrac{1}{\{\dot{x}_T(t_{go}) - \dot{x}_I(t_{go})\}} & 0 & 0 \end{bmatrix} \tag{13}$$

To find the control parameters, the following procedure should be used. First, establish a time to go with zero velocity changes, a good choice being the time to go that yields the

point of closest approach. This time to go is determined by propagating the orbits forward until a minimum relative distance is reached. Because the target is assumed to be in its final boost phase throughout the intercept, this time to go will be less than or equal to the time until ICBM thrust termination. Second, propagate the dynamic equations [Eqs. (1-7)] forward to the intercept time and determine the f vector from Eq. (9). Changes to the control parameters are then obtained from Eq. (12). The velocity changes are applied to the interceptor's initial conditions and the procedure is repeated with the updated time to go until convergence occurs. The resulting control parameters will drive the miss distance to zero with minimum velocity changes. The difference between needed and present velocity are sufficient to determine the interceptor's thrust profile.

Spline Approximations

As discussed earlier, numerical propagation of the dynamic equations is very time consuming. It is convenient to approximate the relative trajectory by a polynomial, eliminating the need for repeated propagation. Cubic splines lend themselves well to this application.[16,22,23] The current and final states can be used to generate cubic splines along each axis of the form

$$x(t) = At^3 + Bt^2 + Ct + D \tag{14}$$

By setting t to zero, D and C become the current position and velocity, respectively, with time to go being the intercept time. Changes in velocity will be reflected only in the C coefficient, and the final state can be determined easily for any intercept time. With this formulation, the determination of the spline coefficients is relatively simple. The current state [let $t = 0$ in Eq. (14)] gives D and C with no computations

$$D = x(o) \tag{15}$$

$$C = \dot{x}(o) \tag{16}$$

The A and B coefficients can be computed using the final states and Eq. (14) as follows:

$$x(t_{go}) = At_{go}^3 + Bt_{go}^2 + Ct_{go} + D \tag{17}$$

$$\dot{x}(t_{go}) = 3At_{go}^2 + 2Bt_{go} + C \tag{18}$$

Because there are only two unknowns in Eqs. (17) and (18), algebraic manipulation yields

$$A = \frac{2[x(o) - x(t_{go})]}{t_{go}^3} + \frac{[\dot{x}(o) + \dot{x}(t_{go})]}{t_{go}^2} \tag{19}$$

$$B = \frac{3[x(t_{go}) - x(o)]}{t_{go}^2} - \frac{[2\dot{x}(o) + \dot{x}(t_{go})]}{t_{go}} \tag{20}$$

There is an added versatility in using splines. Should the system model be changed, only the spline coefficients need be changed. A search algorithm based on the splines will remain the same, operating with the new coefficients. This is very beneficial because recomputing the coefficients is far simpler than altering an algorithm.

To ensure accuracy, new spline coefficients are computed every cycle time. To accomplish this, the truth model is propagated forward to the predicted impact time to obtain the needed final states. By using these updated final states every iteration, propagated roundoff error is eliminated in the spline coefficient computations.

Certainty Control

If the controls associated with cost do not affect state estimate certainty, fuel may be conserved by using that certainty to reduce the controls. By linking the controls to the certainty of the estimate, a near perfect estimate would yield the optimal control, with reduced control resulting from a poor estimate. To accomplish this, the predicted final states are constrained by a function of their variances at the final time. This form of control will be called certainty control and is implemented by establishing the cost function

$$L = \frac{\Delta V_y^2 + \Delta V_z^2}{2} \tag{21}$$

subject to the constraint:

$$f = \frac{\hat{x}_f^2 + \hat{y}_f^2 + \hat{z}_f^2 - K[\sigma_{xf}^2 + \sigma_{yf}^2 + \sigma_{zf}^2]}{2} \le 0 \tag{22}$$

The final state estimates ($\hat{x}_f$, $\hat{y}_f$, $\hat{z}_f$) and their deviations (σ_{xf}, σ_{yf}, σ_{zf}) are determined by running the filter (Appendix A) forward to predicted impact time without measurement or control updates and then representing their time history with splines:

$$x_s = A_x t_{go}^3 + B_x t_{go}^2 + C_x t_{go} + D_x \tag{23}$$

$$y_s = A_y t_{go}^3 + B_y t_{go}^2 + C_y t_{go} + D_y \tag{24}$$

$$z_s = A_z t_{go}^3 + B_z t_{go}^2 + C_z t_{go} + D_z \tag{25}$$

$$\hat{x}_f = x_s \tag{26}$$

$$\hat{y}_f = y_s - \Delta V_y t_{go} \tag{27}$$

$$\hat{z}_f = z_s - \Delta V_z t_{go} \tag{28}$$

$$\sigma_{xf} = A_{\sigma x} t_{go}^3 + B_{\sigma x} t_{go}^2 + C_{\sigma x} t_{go} + D_{\sigma x} \tag{29}$$

$$\sigma_{yf} = A_{\sigma y} t_{go}^3 + B_{\sigma y} t_{go}^2 + C_{\sigma y} t_{go} + D_{\sigma y} \tag{30}$$

$$\sigma_{zf} = A_{\sigma z} t_{go}^3 + B_{\sigma z} t_{go}^2 + C_{\sigma z} t_{go} + D_{\sigma z} \tag{31}$$

Conceptually, the constraint produces a deviation sphere about the predicted impact point. If the predicted miss is inside or touching the sphere, thrusting is not necessary. If the predicted miss is outside the sphere, minimum thrusting is determined to bring the miss to the surface of the sphere. As the estimates improve, the constraint tightens and the sphere shrinks. The spline representations allow this stochastic problem to be solved deterministically. The constraint is adjoined via a Lagrange multiplier to the cost function to form the Hamiltonian[25]

$$H = L + \lambda f \tag{32}$$

To minimize the cost L while satisfying the constraint f, the partials of H with respect to the controls must equal zero

$$\frac{\partial H}{\partial \Delta V_y} = \Delta V_y - \lambda \hat{y}_f t_{go} = 0 \tag{33}$$

$$\frac{\partial H}{\partial \Delta V_z} = \Delta V_z - \lambda \hat{z}_f t_{go} = 0 \tag{34}$$

$$\frac{\partial H}{\partial t_{go}} = \lambda(\hat{x}_f \dot{\hat{x}}_f + \hat{y}_f \dot{\hat{y}}_f + \hat{z}_f \dot{\hat{z}}_f - K[\sigma_{xf}\dot{\sigma}_{xf} + \sigma_{yf}\dot{\sigma}_{yf} + \sigma_{zf}\dot{\sigma}_{zf}]) = 0 \tag{35}$$

with the dot term expansions computed in Appendix B.

Equations (22), (33), (34), and (35) constitute four equations with four unknowns, which can be reduced to two equations and two unknowns using Eqs. (27) and (28). Substituting Eq. (27) into Eq. (33) yields

$$\Delta V_y = \frac{\lambda y_s t_{go}}{1 + \lambda t_{go}^2} \tag{36}$$

$$\hat{y}_f = \frac{y_s}{1 + \lambda t_{go}^2} \tag{37}$$

In a similar manner, substituting Eq. (28) into Eq. (34) yields

$$\Delta V_z = \frac{\lambda z_s t_{go}}{1 + \lambda t_{go}^2} \tag{38}$$

$$\hat{z}_f = \frac{z_s}{1 + \lambda t_{go}^2} \tag{39}$$

Equations (22) and (35) can now be solved in terms of λ and t_{go}. Once known, ΔV_y and ΔV_z can be determined from Eqs. (36) and (38). The parameters λ and t_{go} can be found by numerical techniques using the Jacobian

$$[J] \begin{bmatrix} dt_{go} \\ d\lambda \end{bmatrix} = \begin{bmatrix} -f_1 \\ -f_2 \end{bmatrix} \tag{40}$$

$$f_1 = \frac{\hat{x}_f^2 + \hat{y}_f^2 + \hat{z}_f^2 - K[\sigma_{xf}^2 + \sigma_{yf}^2 + \sigma_{zf}^2]}{2} \tag{41}$$

$$f_2 = \hat{x}_f\dot{\hat{x}}_f + \hat{y}_f\dot{\hat{y}}_f + \hat{z}_f\dot{\hat{z}}_f - K[\sigma_{xf}\dot{\sigma}_{xf} + \sigma_{yf}\dot{\sigma}_{yf} + \sigma_{zf}\dot{\sigma}_{zf}] \tag{42}$$

with the elements of the Jacobian matrix computed in Appendix B.

Should the states be perfectly known, the σ terms will be zero. In this case, the equations for certainty control reduce to those of optimal control formulation. Should the estimate be poor, the σ terms will be large and the inequality constraint of Eq. (22) is met with very little (if any) change in velocity. This demonstrates the principle of certainty control, where the certainty of the estimate affects control energy expenditure.

Algorithm

1) Propagate EKF forward one time step without measurement or control updates and get new state estimates, $\hat{x}(0)$, and variances, $\hat{\sigma}(0)$, for next time step. Use the secant method to approximate $\hat{x}(0)$ and $\dot{\hat{\sigma}}(0)$.

2) Reset t_{go} to $(t_{go} - 0.1)$ to account for advanced step from step 1 (this paper uses a time step of 0.1 s).

3) Propagate EKF forward to intercept time (t_{go}) without updates to get $\hat{x}(t_{go})$ and $\hat{\sigma}(t_{go})$.

4) Reset EKF to current time.

5) Determine the spline equations for $\hat{x}(t)$ and $\hat{\sigma}(t)$ using the data from steps 1 and 3.

6) Determine the lateral velocity changes and new intercept time using certainty control. In other words, minimize

$$L = \frac{\Delta V_y^2 + \Delta V_z^2}{2}$$

subject to the constraint

$$f = \frac{\hat{x}_f^2 + \hat{y}_f^2 + \hat{z}_f^2 - K[\sigma_{xf}^2\sigma_{yf} + \sigma_{zf}^2]}{2} \le 0$$

where the subscript f denotes the final state at the new intercept time. (It is not necessary to use splines to do this step. We chose splines to reduce computational burdens and allow a solution that lends itself to deterministic techniques. The estimates and variances in the constraint equation make this problem stochastic, but by approximating them with spline equations where time becomes a variable, a deterministic approach to the solution can be used.)

7) Reset t_{go} to the new intercept time and apply the velocity changes from step 6. If the velocity change in a given axis is below the minimum threshold, then do not apply the computed ΔV in that axis. Minimum threshold for this paper was 0.3 m/s (3.0 m/s^2 × 0.1 s time step). Maximum ΔV for any axis is 60 m/s^2. If ΔV exceeds this limit, it is reset to the limit.

8) Now advance one time step. Propagate and update the EKF with the next set of sensor observations and return to step 1 of this algorithm.

Computer Simulation

Two cases are examined with time to go equaling 30 s. Case 1 represents a head-on, 10-deg out-of-plane intercept, and case 2 represents a 10-deg out-of-plane tail chase. The interceptor is initially traveling at 12 km/s at an altitude of 750 km with a lateral acceleration range of 3-60 m/s^2 in each axis. The booster's initial acceleration is 3.15788 m/s^2 with a unitized mass flow rate of 0.01579 s^{-1}.

A time lag of 0.1 s is used for all algorithms when computing velocity changes. It is unrealistic to assume that the filter can process measurements, the controller determine thrust commands, and the thrusters respond to those commands all instantaneously. One cycle time is chosen to allow the velocity changes computed in the previous cycle to be implemented in the present cycle. The controller routines are built to take this lag into account. Also, thrusting is not permitted during the first 3 s of an intercept to account for target acquisition. This simulation, written in Fortran 77 to run on a Vax 8600, generates 100 Monte Carlo runs per case.

Results

Seven algorithms were programmed to serve as a basis of comparison with the certainty control algorithm. Plan A uses the cost function incorporating velocity changes and miss distance weighted by a weighting factor K ($K = 10$ for this simulation).

$$L = \frac{x_f^2 + y_f^2 + z_f^2}{2} + \frac{\Delta V_y^2 + \Delta V_z^2}{2} \tag{43}$$

Plan B uses the same loss function but with $K = \infty$, a zero miss solution. Plan C uses a proportional navigation scheme recognizing that the velocity vector on the target is changing.

The next plan is an optimal spacing algorithm where control is applied based on control effectiveness.[28] Corrective thrusting is applied when the control has $(1/\rho)$ the effect of the previous corrective thrust. A value of $\rho = 1.75$ was determined during the simulation of plan B to be the best value. The dual control algorithm[5] minimizes the expected value of Eq. (43) or

$$E\{L\} = K\left[\frac{\sigma_{xf}^2 + \sigma_{yf}^2 + \sigma_{zf}^2}{2} + \frac{\hat{x}_f^2 + \hat{y}_f^2 + \hat{z}_f^2}{2}\right] + E\left[\frac{\Delta V_y^2 + \Delta V_z^2}{2}\right] \tag{44}$$

Table 1. Case 1 performance head-on, 10-deg out-of-plane intercept

	Mean miss, m	Standard deviation, m	Mean ΔV, m/s	Standard deviation, m/s
Plan A, $K = 10$ (CE optimal)	0.502	0.224	83.82	6.99
Plan B, $K = \infty$ (CE optimal)	0.360	0.171	90.39	7.24
Plan C (PRO NAV)[a]	0.360	0.171	93.07	7.39
Optimum spacing, $\rho = 1.75$	0.361	0.171	37.19	8.50
Dual control, $K = 10$	0.501	0.224	83.82	6.99
Certainty control, $K = 0.4$	0.386	0.191	23.21	4.18
Truth with noise	0.545	0.264	83.69	7.18
Truth without noise	0	na	7.54	na

[a]Proportional navigation.

The next algorithm is that of certainty control presented in this paper. The last two are truth models with and without noise. The performance of the truth model vs the various algorithms is recorded in Tables 1 and 2.

The data indicates the dual control's performance is no better than the certainty equivalence formulation of plan A. This is due to the fact that range is included as a measurement, causing the control to have virtually no effect on improving filter variance. Plan B is more accurate than plan A, but more costly in energy. Again, this result is expected because the formulation of plan B is based on infinite miss penalty ($K = \infty$) for plan A. By optimally spacing the thrusts of plan B, energy expenditure is considerably reduced with little or no sacrifice in accuracy.

Table 2. Case 2 performance 10-deg out-of-plane tail chase

	Mean miss, m	Standard deviation, m	Mean ΔV, m/s	Standard deviation, m/s
Plan A, $K = 10$ (CE optimal)	0.190	0.100	129.61	13.29
Plan B, $K = \infty$ (CE optimal)	0.126	0.061	132.65	13.32
Plan C (PRO NAV)[a]	0.126	0.061	129.47	12.26
Optimum spacing, $\rho = 1.75$	0.126	0.059	39.96	12.85
Dual control, $K = 10$	0.190	0.100	129.61	13.29
Certainty control, $K = 0.4$	0.136	0.076	29.74	9.10
Truth with noise	0.379	0.204	123.57	11.61
Truth without noise	0	na	9.52	na

[a]Proportional navigation.

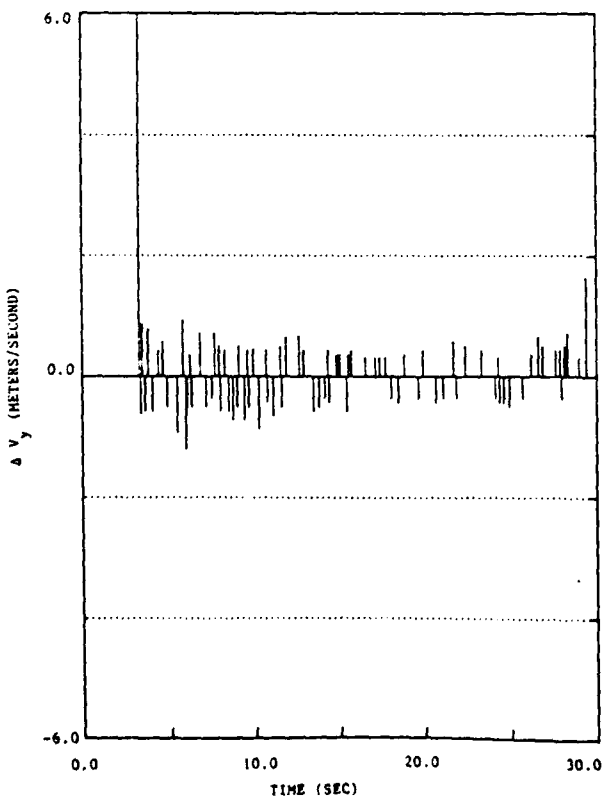

Fig. 1 In-plane thrust profile of truth model for case 1.

Plan C is just as accurate as plan B, with slightly greater cost resulting from large initial intercept range. This extra cost is attributed to the negligible gravity assumption used in the formulation of plan C. For the smaller ranges associated with a tail chase, plan C was actually less costly than plan B.

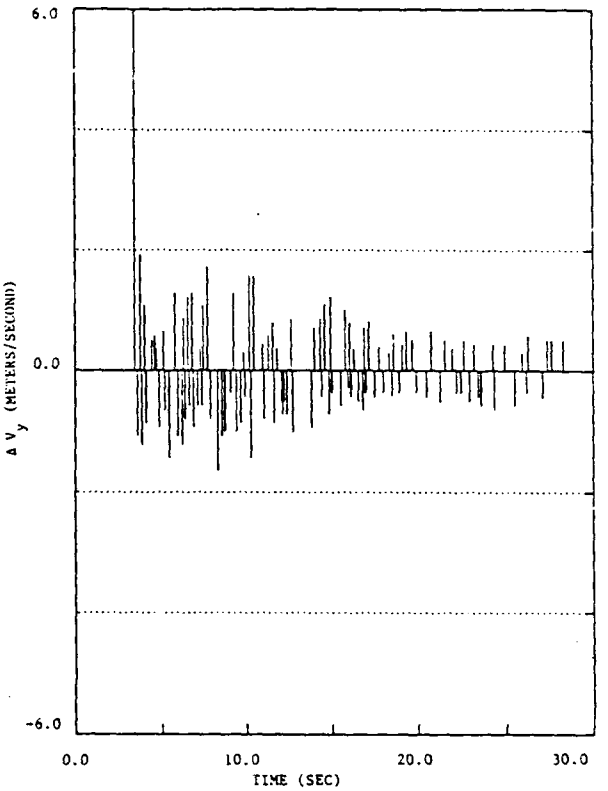

Fig. 2 In-plane thrust profile of truth model for case 2.

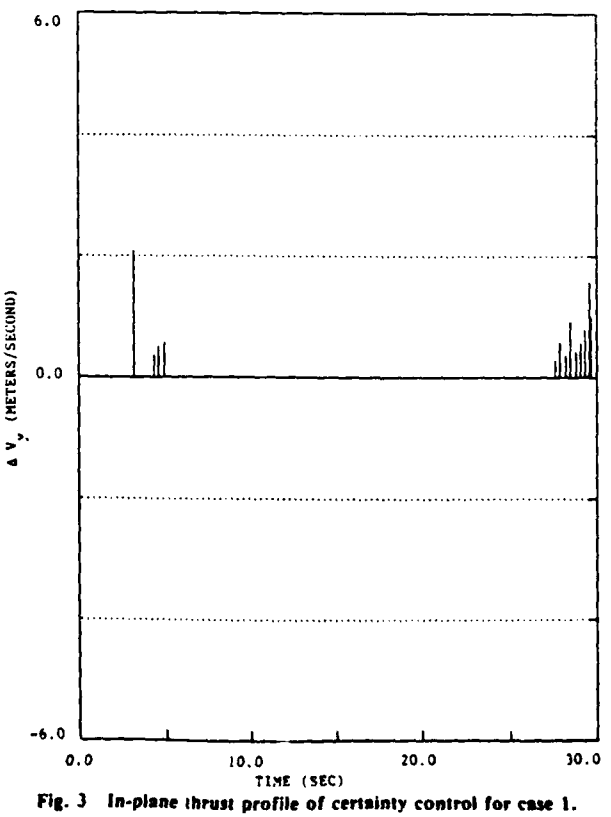

Fig. 3 In-plane thrust profile of certainty control for case 1.

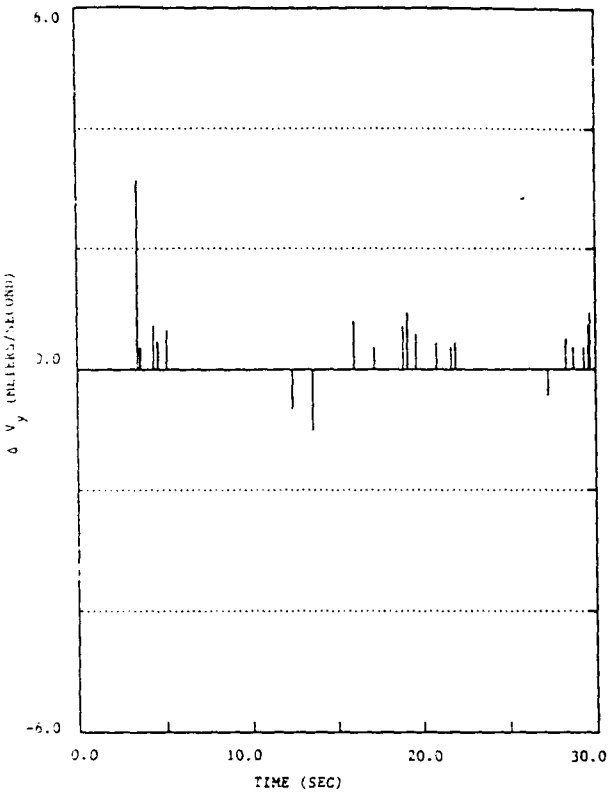

Fig. 4 In-plane thrust profile of certainty control for case 2.

The effect of estimate uncertainty can be observed from the truth model in-plane thrust profiles (Figs. 1 and 2). This uncertainty causes needless and often counterproductive thrusting. In contrast, certainty control requires considerably less energy expenditure (Figs. 3 and 4). This result is not surprising, as the formulation of certainty control is based on reducing control energy in the presence of poor estimates. This form of control works well because filter variance is range dependent. As range decreases, the control constraint tightens and accuracy increases. Therefore, less fuel is used when range is great and estimates are poor, with refinements made as impact nears.

Conclusions

In this paper, six guidance schemes were examined to determine their capability to minimize lateral velocity changes of a hypervelocity orbital intercept vehicle. Optimal control using certainty equivalence (plans A and B), proportional navigation (plan C), control with optimum thrust spacing, dual control, and certainty control were all implemented for two cases.

Certainty control can be effective in reducing energy expenditure when the controls associated with cost do not affect state estimate certainty. If the controls can improve the estimate, then dual control techniques may be more effective in reducing cost. Because range is included as a measurement, lateral deviations do not noticeably improve the estimate, allowing certainty control to significantly reduce thrusting.

Certainty control contrains the final condition to a function of final estimator accuracy in the absence of updates. This general approach is not limited to hypervelocity vehicles and would suggest other applications of this form to control intercepts stochastically.

Dual control requires a measure of final estimator accuracy, which was achieved by running the extended Kalman filter forward to intercept time without updates. This time-consuming process could be eliminated if filter variances could be estimated by some function (polynomial or otherwise). Also, the constraint multiplier was assumed constant for this formulation. A future area of research is to develop a multiplier that is range or time dependent to further reduce interceptor thrusting.

In summary, the approach identified by this research not only improves the efficiency of hypervelocity intercept, but can be applied to a broad range of stochastic problems where control energy does not improve filter accuracy. It is also possible to combine the effects of dual and certainty control in certain cases by initially using dual control to improve estimator accuracy and then switching to certainty control. Endgame accuracy may be improved by switching from certainty control to a certainty equivalence formulation just prior to impact.

Appendix A: Extended Kalman Filtering

Optimal estimates of the interceptor and target are needed for the search algorithms to converge properly. Because of the nature of the dynamics and sensors, the relative position and velocity must be estimated from sampled nonlinear measurements. The estimation problem for a nonlinear system having continuous dynamics and discrete-time measurements is addressed by Gelb.[26] The EKF was chosen over other estimation methods because the optimal estimate is determinate. That is, the dynamics and observations of the interceptor and target can be well predicted in the presence of Gaussian noise. The EKF states are defined from Eqs. (5-11) as follows:

$$x_1 = x_T - x_I \tag{A1}$$

$$x_2 = \dot{x}_T - \dot{x}_I \tag{A2}$$

$$x_3 = y_T - y_I \tag{A3}$$

$$x_4 = \dot{y}_T - \dot{y}_I \tag{A4}$$

$$x_5 = z_T - z_I \tag{A5}$$

$$x_6 = \dot{z}_T - \dot{z}_I \tag{A6}$$

$$x_7 = A \tag{A7}$$

$$x_8 = \dot{m} \tag{A8}$$

The measurements of range and LOS angles are

$$z_1(k) = \sqrt{x_1^2 + x_3^2 + x_5^2} + V_R(k) \tag{A9}$$

$$z_2(k) = \tan^{-1}(x_5/x_9) + V_6(k) \tag{A10}$$

$$z_3(k) = \tan^{-1}(x_3/x_1) + V_R(k) \tag{A11}$$

It is advantageous to process measurements one at a time. This method, called serial updating,[27] eliminates the requirement to compute a matrix inverse, thereby reducing computer load and avoiding the computational problems associated with inverting an ill-conditioned matrix. Also, measurements may be skipped without reformulating the filter equations, allowing greater flexibility in examining various tracking schemes. The simultaneous components of the measurement vector z_k can be considered serially over a very short time span. The propagation noise w stems from using a fourth-order Runge-Kutta integrator with updates every 0.1 s on a 64-bit word.

$$w_{x,y,z}(t) \sim N(0,\ 2.21516 \times 10^{-18}\ \mathrm{m^2/s})$$

$$w_{\dot{x},\dot{y},\dot{z}}(t) \sim N(0,\ 5.52049 \times 10^{-20}\ \mathrm{m^4/s^3})$$

$$w_A(t) \sim N(0,\ 4.29831 \times 10^{-12}\ \mathrm{m^2/s^5})$$

$$w_m(t) \sim N(0,\ 2.493241 \times 10^{-7}\ 1/\mathrm{s^3})$$

In all cases, the measurement ν noise properties associated with the filter are

$$V_{\theta,\gamma}(k) \sim N(0,\ 1.0 \times 10^{-8})$$

$$V_R(k) \sim N(0,\ 1.0 \times 10^{-8} \times R^2\ \mathrm{m}^2)$$

where θ is the out-of-plane, line-of-sight angle, γ the in-plane line-of-sight angle, and R the range.

The startup variances for all runs are

$$\sigma^2_{xx} = \sigma^2_{yy} = \sigma^2_{zz} = 100\ \mathrm{m}^2$$

$$\sigma^2_{\dot{x}\dot{x}} = \sigma^2_{\dot{y}\dot{y}} = \sigma^2_{\dot{z}\dot{z}} = 10\ \mathrm{m}^2/\mathrm{s}^2$$

$$\sigma^2_{AA} = 0.1\ \mathrm{m}^2/\mathrm{s}^4$$

$$\sigma^2_{mm} = 2.493241 \times 10^{-6}\ \mathrm{s}^{-2}$$

Appendix B: Derivation of Certainty Control Equations

The dot terms for Eq. (39) are computed as follows:

$$\dot{x}_f = 3A_x t_{go}^2 + 2B_x t_{go} + C_x \tag{B1}$$

$$\dot{y}_f = 3A_y t_{go}^2 + 2B_y t_{go} + C_y - \Delta V_y \tag{B2}$$

$$\dot{z}_f = 3A_z t_{go}^2 + 2B_z t_{go} + C_z - \Delta V_z \tag{B3}$$

$$\dot{\sigma}_{xf} = 3A_{\sigma x} t_{go}^2 + 2B_{\sigma x} t_{go} + C_{\sigma x} \tag{B4}$$

$$\dot{\sigma}_{yf} = 3A_{\sigma y} t_{go}^2 + 2B_{\sigma y} t_{go} + C_{\sigma y} \tag{B5}$$

$$\dot{\sigma}_{zf} = 3A_{\sigma z} t_{go}^2 + 2B_{\sigma z} t_{go} + C_{\sigma z} \tag{B6}$$

The Jacobian matrix elements for Eq. (44) are

$$J_{11} = \frac{\partial f_1}{\partial t_{go}} = f_2 \tag{B7}$$

$$J_{12} = \frac{\partial f_1}{\partial \lambda} = \hat{y}_f \frac{\partial \hat{y}_f}{\partial \lambda} + \hat{z}_f \frac{\partial \hat{z}_f}{\partial \lambda} \tag{B8}$$

$$\frac{\partial \hat{y}_f}{\partial \lambda} = \frac{-y_s t_{go}^2}{(1 + \lambda t_{go}^2)^2} \tag{B9}$$

$$\frac{\partial \hat{z}_f}{\partial \lambda} = \frac{-z_s t_{go}^2}{(1 + \lambda t_{go}^2)^2} \tag{B10}$$

$$J_{21} = \frac{\partial f_2}{\partial t_{go}} = \hat{x}_f \ddot{\hat{x}}_f + \dot{\hat{x}}_f^2 + \hat{y}_f \ddot{\hat{y}}_f + \dot{\hat{y}}_f^2 + \hat{z}_f \ddot{\hat{z}}_f + \dot{\hat{z}}_f^2 - K[\sigma_{xf}\ddot{\sigma}_{xf} + \dot{\sigma}_{xf}^2 + \sigma_{yf}\ddot{\sigma}_{yf} + \dot{\sigma}_{yf}^2 + \sigma_{zf}\ddot{\sigma}_{zf} + \dot{\sigma}_{zf}^2] \tag{B11}$$

$$\ddot{\hat{x}}_f = 6A_{ox} t_{go} + 2B_x \tag{B12}$$

$$\ddot{\hat{y}}_f = 6A_y t_{go} + 2B_y - \lambda(\dot{\hat{y}}_f t_{go} + \hat{y}_f) \tag{B13}$$

$$\ddot{\hat{z}}_f = 6A_z t_{go} + 2B_z - \lambda(\dot{\hat{z}}_f t_{go} + \hat{z}_f) \tag{B14}$$

$$\ddot{\sigma}_{xf} = 6A_{\sigma x} t_{go} + 2B_{\sigma x} \tag{B15}$$

$$\ddot{\sigma}_{yf} = 6A_{\sigma y} t_{go} + 2B_{\sigma y} \tag{B16}$$

$$\ddot{\sigma}_{zf} = 6A_{\sigma z} t_{go} + 2B_{\sigma z} \tag{B17}$$

$$J_{22} = \frac{\partial f_2}{\partial \lambda} = \frac{\partial \hat{y}_f}{\partial \lambda} \dot{\hat{y}}_f + \hat{y}_f \frac{\partial \dot{\hat{y}}_f}{\partial \lambda} + \frac{\partial \hat{z}_f}{\partial \lambda} \dot{\hat{z}}_f + \hat{z}_f \frac{\partial \dot{\hat{z}}_f}{\partial \lambda} \tag{B18}$$

$$\frac{\partial \dot{\hat{y}}_f}{\partial \lambda} = -\frac{y_s t_{go}}{(1 + \lambda t_{go}^2)^2} \tag{B19}$$

$$\frac{\partial \dot{\hat{z}}_f}{\partial \lambda} = -\frac{z_s t_{go}}{(1 + \lambda t_{go}^2)^2} \tag{B20}$$

References

[1]Guelman, M., "Qualitative Study of Proportional Navigation," *IEEE Transactions on Aerospace and Electronic Systems*, Vol. AES-7, No. 4, 1971, pp. 337–343.

[2]Guelman, M., "The Closed Form Solution of Pure Proportional Navigation," *IEEE Transactions on Aerospace and Electronic Systems*, Vol. AES-12, No. 4, 1976, pp. 472–482.

[3]Sridhar, B., and Gupta, N. K., "Missile Guidance Laws Based on Singular Perturbation Methodology," *Journal of Guidance and Control*, Vol. 3, April 1980, pp. 158–166.

[4]Tse, E., Bar-Shalom, Y., and Meier, L., III, "Wide Sense Adaptive Dual Control for Nonlinear Stochastic Systems," *IEEE Transactions on Automatic Control*, Vol. AC-18, No. 2, 1973, pp. 98–108.

[5]Tse, E., and Bar-Shalom, Y., "Adaptive Dual Control for Stochastic Nonlinear Systems with Free End-Time," *IEEE Transactions on Automatic Control*, Oct. 1975, pp. 670–675.

[6]Nesline, F. W., Wells, B. H., and Zachran, P., "Combined Optimal/Classic Approach to Robust Missile Autopilot Design," *Journal of Guidance and Control*, Vol. 4, No. 3, 1981, pp. 316–322.

[7]Speyer, J. L., Hull, D. G., and Tseng, C. Y., "Estimation Enhancement by Trajectory Modulation for Homing Missiles," *Journal of Guidance, Control, and Dynamics*, Vol. 7, No. 2, 1984, pp. 167–174.

[8]Guelman, M., and Shinar, J., "Optimal Guidance Law in the Plane," *Journal of Guidance, Control, and Dynamics*, Vol. 7, No. 4, 1984, pp. 471–476.

[9]Tang, Y. M., and Borrie, J. A., "Missile Guidance Based on Kalman Filter Estimation of Target Maneuver," *IEEE Transactions on Aerospace and Electronic Systems*, Vol. AES-20, No. 6, 1984, pp. 736–741.

[10]Yeuh, W. R., and Lin, C. F., "Optimal Controller for Homing Missile," *Journal of Guidance, Control, and Dynamics*, Vol. 8, No. 3, 1985, pp. 408–411.

[11]Lin, C. F., and Lee, S. P., "Robust Missile Autopilot Design Using a Generalized Singular Optimal Control Technique," *Journal of Guidance, Control, and Dynamics*, Vol. 8, No. 4, 1985, pp. 498–507.

[12]Ashida, S., Howe, R. M., and Vinh, N. X., "Optimal Control of Air-Launched Homing Missiles Based on Realistic Performance Indices," *Proceedings of the Conference on Aerospace Simulation II*, Vol. 16, No. 2, 1986, pp. 179–186.

[13]Lin, C. F., and Tsai, L. L., "Analytical Solution of Optimal Trajectory-Shaping Guidance," *Journal of Guidance, Control, and Dynamics*, Vol. 10, No. 1, 1987, pp. 61–66.

[14]Yang, C. D., and Yeh, F. B., "Closed-Form Solution for a Class of Guidance Laws," *Journal of Guidance, Control, and Dynamics*, Vol. 10, No. 4, 1987, pp. 412–415.

[15]Cherry, G. W., "A General, Explicit, Optimizing Guidance Law for Rocket-Propelled Spaceflight," AIAA Paper 64-638, Aug. 1964.

[16]Johnson, F. T., "Approximate Finite-Thrust Trajectory Optimization," *AIAA Journal*, Vol. 7, No. 6, 1969, pp. 993–997.

[17]Bate, R. R., Mueller, D. C., and White, J. E., *Fundamentals of Astrodynamics*, Dover, New York, 1971.

[18]Borisenko, I. I., and Kulyabichev, Y. P., "Algorithm for Optimization of the Solution of the Spacecraft Rendezvous Problem," *Cosmic Research*, Vol. 18, No. 3, 1980, pp. 343–347.

[19]Stuart, D. G., "A Simple Targeting Technique for Two-Body Spacecraft Trajectories," *Journal of Guidance, Control, and Dynamics*, Vol. 9, No. 1, 1986, pp. 27–31.

[20]Bhat, M. S., and Shrivastava, S. K., "An Optimal Q-Guidance Scheme for Satellite Launch Vehicles," *Journal of Guidance, Control, and Dynamics*, Vol. 10, No. 1, 1987, pp. 53–60.

[21]Menon, P. K. A., and Calise, A. J., "Interception, Evasion, Rendezvous and Velocity-to-Be-Gained Guidance for Spacecraft," AIAA Paper 87-2318, Aug. 1987.

[22]Dickmanns, F. D., and Wells, K. H., "Approximate Solution of Optimal Control Problems Using Third Order Hermite Polynomial Functions," *Proceedings of the 6th Technical Conference on Optimization Techniques*, Springer-Verlag, New York, 1975.

[23]Hargraves, C. R., and Paris, S. W., "Direct Trajectory Optimization Using Nonlinear Programming and Collocation," *Journal of Guidance, Control, and Dynamics*, Vol. 10, No. 4, 1987, pp. 338–342.

[24]Maron, M. J., *Numerical Analysis: A Practical Approach*, Macmillan, New York, 1982, pp. 177–182.

[25]Bryson, A. E., and Ho, Y. C., *Applied Optimal Control*, Hemisphere, Washington, DC, 1975, pp. 71–75.

[26]Gelb, A., *Applied Optimal Estimation*, Massachusetts Institute of Technology Press, Cambridge, MA, 1986, pp. 180–228.

[27]Ho, Y. C., "On the Stochastic Approximation Method and Optimal Filtering Theory," *Journal of Mathematical Analysis and Applications*, Vol. 6, 1963, pp. 152–154.

[28]Leitmann, G., *Optimization Techniques*, Academic, New York, 1962, pp. 353–357.